ATTITUDE STABILIZATION OF AN UNKNOWN AND SPINNING TARGET SPACECRAFT USING A VISCO-ELASTIC TETHER

Kirk Hovell and Steve Ulrich

Carleton University, Ottawa, Ontario, K1S5B6, Canada

ABSTRACT

Active removal of large de-commissioned satellites is critical to the continued use of many of Earth's orbits, as predicted by Donald J. Kessler in 1976. One solution to this problem is to use a tethered spacecraft system to capture and tow the highest risk debris to a disposal orbit. A significant technical challenge lies with the capture of and subsequent stabilization of a large and possibly tumbling debris. This paper addresses the target attitude stabilization aspect of the capture process. The system analyzed consists of a single tether attached to the active chaser spacecraft, which branches into four sub-tethers attached to the debris. Incorporating the thrust ability of the chaser and exploiting the visco-elastic properties of the tethers, it was shown through numerical simulation that the proposed novel tethered spacecraft configuration provides a means of controlling the attitude of an uncooperative debris.

Key words: Tether; Capture; Space debris, Attitude motion.

1. INTRODUCTION

The density of Earth-orbiting debris has increased dramatically over the last decade. The highest risk debris are the largest (e.g., non-cooperative decommissioned satellites), which, in the event of a collision have the potential to create many additional debris. It is foreseen that if the number of debris keeps increasing with the current growth rate, this will rapidly lead to an exponential growth in collisions (referred to as the *Kessler Syndrome*), thereby reducing the availability of some orbits due to the higher risk of collision with orbiting space debris. In this context, controlling the growth of the large space debris population is a high-priority task of the world's major space agencies.

To address this contemporary problem, several space debris mitigation approaches were recently proposed. One of the most promising solutions consists of a tethered spacecraft system (TSS), i.e., an active "chaser" spacecraft capturing and deorbiting a non-cooperative, and possibly spinning, "target" spacecraft (i.e., a space debris) using a viscous-elastic tether [1]. However, the use of tethered spacecraft systems to remove space debris from populated orbits involves several technical challenges. Those challenges are mostly related to the structural flexibility of the tether coupled with the large angular velocities of space debris that may exceed 30 rotations per minute [2]. For this reason, controlling the relative dynamics of the chaser spacecraft with respect to the target spacecraft, in such a way that the flexible tether dissipates the angular momentum of the debris, is critical to ensuring the success of the TSS debris-removal technological solution. Indeed, only once the angular momentum of the debris is damped out, can the chaser safely maneuver without risk of collision.

Tethered spacecraft systems are fairly common (e.g., extensively used for spacewalks), and therefore have been studied in-depth [3]. However, in these studies, both objects, attached together by a tether, were treated as point masses. This is sufficient detail when each object has a means of controlling its own attitude (as is present during a spacewalk or other applications). However, in in the context of using one spacecraft to control a spinning and uncooperative space debris, a more detailed analysis on the attitude dynamics of the debris must be considered.

The effect a TSS has on an the attitude of an uncooperative target has been studied by Aslanov and Yudintsev [4]. Here, a Lagrangian approach was taken to model the two-dimensional dynamics of a tether on a rigid passive target. Numerical simulations were performed for various cases, which concluded that a tether is feasible for controlling a spinning target. It was also found that a slack tether should be avoided, as it can yield high amplitude oscillations of the target attitude about its equilibrium point.

A Lagrangian approach to model the TSS effects on a rigid target with flexible appendages was performed in [5] (in two-dimensions) and [6] (in three-dimensions). It was found that the tether material properties (i.e., stiffness) must be selected such that it does not generate TSS oscillations that coincide with the natural frequencies of the target spacecraft when the flexible appendages are deployed. The effect of flexible appendages is not considered in this paper.

Aslanov and Yudintsev [7] further modeled the TSS using

a three-dimensional Newtonian approach. More representative effects such as orbital motion, gravity-gradient torques, and atmospheric drag were included in the simulations. Certain configurations were found to lead to safe transportation, such as when the tether is aligned with the thrust force from the chaser. It was found that sufficient levels of thrust force are required from the chaser, and this level increases as the altitude of the TSS decreases due to the increasing effect of atmospheric drag (described in more detail in [8]). Most notably, it was found that tether damping only slightly reduces the attitude oscillations of the passive satellite. Therefore, the target spacecraft will be oscillating during the deorbiting period, possibly leading to control difficulties for the chaser.

In this context, this paper proposes a novel tethered spacecraft configuration to dramatically improve the attitude stabilizing ability of the TSS. The novel approach is to implement four sub-tethers attached to the debris at various locations to increase its attitude stability. Similar to [7], a three-dimensional Newtonian modeling approach is taken. Dynamics formulations and simulations are presented to demonstrate the feasibility of this novel technique.

This paper is organized as follows: Section 2 describes the approach taken to solve the dynamics problem, Section 3 presents a dynamics formulation, Section 4 demonstrates the feasibility of the approach using numerical simulations, and Sections 5 and 6 discuss and summarize the results.

2. APPROACH

The tethered spacecraft system (TSS) consists of an active satellite (chaser) connected to a debris (target) via a visco-elastic tether. The tether is attached to the chaser and branches into four sub-tethers at a certain point on the tether (denoted "junction"). The four sub-tethers then attach to the extremities of the chaser-facing side of the target. The single tether leaving the chaser will be denoted as the "main tether" and the four tethers connecting the main tether to the target are denoted as "sub-tethers". The approach taken herein is to use the spring-damper properties of the main tether and sub-tethers to regulate the angular momentum of an uncontrolled target.

Referring to Fig. 1, the reference frame $\mathcal{F}_\mathrm{I}$ represents an inertially fixed reference frame. The position of the target is described by position vector $\vec{\mathbf{r}}_\mathrm{t}$, where:

$$\vec{\mathbf{r}}_\mathrm{t} = \vec{\mathcal{F}}_\mathrm{I}^\mathrm{T} \mathbf{r}_\mathrm{t} \tag{1}$$

Here, $\mathbf{r}_\mathrm{t}$ represents the three-dimensional components of the target centre of mass vector in the inertially fixed reference frame $\mathcal{F}_\mathrm{I}$. The junction and chaser are represented as point masses, their locations described by position vectors $\vec{\mathbf{r}}_\mathrm{c}$ and $\vec{\mathbf{r}}_\mathrm{j}$, respectively, such that:

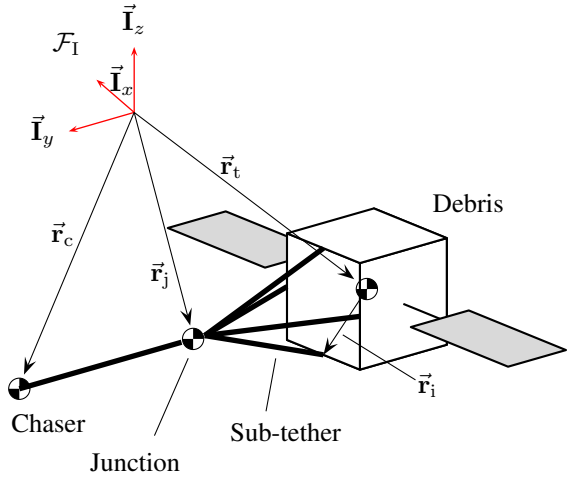

Figure 1. Reference frame and vector definition for modeling sub-tether effects.

$$\vec{\mathbf{r}}_\mathrm{c} = \vec{\mathcal{F}}_\mathrm{I}^\mathrm{T} \mathbf{r}_\mathrm{c} \tag{2}$$

$$\vec{\mathbf{r}}_\mathrm{j} = \vec{\mathcal{F}}_\mathrm{I}^\mathrm{T} \mathbf{r}_\mathrm{j} \tag{3}$$

where $\mathbf{r}_\mathrm{c}$ and $\mathbf{r}_\mathrm{j}$ are the three-dimensional components of the chaser and junction vectors in the inertially fixed reference frame $\mathcal{F}_\mathrm{I}$, respectively.

Assuming that the target body-fixed frame, $\mathcal{F}_\mathrm{B}$, is aligned with the principal axis of the body, the target inertia matrix is represented by:

$$\mathbf{I} = \begin{bmatrix} I_{xx} & 0 & 0 \\ 0 & I_{yy} & 0 \\ 0 & 0 & I_{zz} \end{bmatrix} \tag{4}$$

where I_{xx}, I_{yy}, and I_{zz} are the principal moments of inertia of the target debris.

3. DYNAMICS FORMULATION

Euler's equations of motion are used to describe the target angular rates, given by [9]:

$$\mathbf{I}\dot{\boldsymbol{\omega}} + \boldsymbol{\omega}^\times(\mathbf{I}\boldsymbol{\omega}) = \mathbf{T} \tag{5}$$

where $\boldsymbol{\omega}$ is the components of the angular rate vector in the target body-fixed frame, $\mathbf{T}$ is the external torque applied to the target, and $\mathbf{I}$ is the inertia matrix.

The attitude of the target is described by quaternion kinematics, given by:

$$\dot{\mathbf{q}} = \frac{1}{2}\mathbf{q}\boldsymbol{\omega} \tag{6}$$

Here, $\mathbf{q}$ represents the quaternion describing the attitude of $\mathcal{F}_{\mathrm{B}}$ with respect to $\mathcal{F}_{\mathrm{I}}$ and is defined as [9]:

$$\mathbf{q} = \begin{bmatrix} q_1 \\ q_2 \\ q_3 \\ q_4 \end{bmatrix} = \begin{bmatrix} \mathbf{b}\cos(\frac{\phi}{2}) \\ \sin(\frac{\phi}{2}) \end{bmatrix} \tag{7}$$

where $\mathbf{b}$ is the axis describing the rotation and ϕ is the angle of rotation.

To model the target, junction, and chaser linear motion, Newton's second law is used:

$$\mathbf{F} = m\mathbf{a} \tag{8}$$

where $\mathbf{F}$ is the net external force applied to the body, m is the mass of the body, and $\mathbf{a}$ is the linear acceleration.

In the TSS, it is the main tether and sub-tethers that are generating the external forces and torques applied to each mass. The tether is modeled as a simple spring-damper system, as shown in Fig. 2.

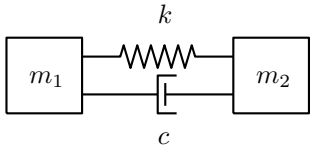

Figure 2. Simple spring-damper system, where two masses are attached via a spring and damper in parallel.

Defining the i^{th} sub-tether under analysis by the vector $\vec{\mathbf{L}}_{\mathrm{i}}$ in the inertially fixed reference frame as having components of:

$$\mathbf{L}_{\mathrm{i}} = \mathbf{r}_{\mathrm{j}} - \mathbf{r}_{\mathrm{t}} - \mathbf{A}(\mathbf{q})^{\mathrm{T}}\mathbf{r}_{\mathrm{i}}, \qquad \forall\, \mathrm{i} = 1, ..., 4 \tag{9}$$

where $\mathbf{r}_{\mathrm{i}}$ is the attachment point of the sub-tether to the target, with respect the the centre of the target, in the target body-fixed reference frame. The rotation matrix $\mathbf{A}(\mathbf{q})$ represents a rotation from the inertially fixed reference frame to the target-fixed reference frame, i.e.,

$$\mathbf{A}(\mathbf{q}) = \vec{\mathcal{F}}_{\mathrm{B}}\vec{\mathcal{F}}_{\mathrm{I}}^{T}, \tag{10}$$

and is obtained from the quaternion through

$$\mathbf{A}(\mathbf{q}) = \begin{bmatrix} 1-2q_2^2-2q_3^2 & 2(q_1q_2+q_4q_3) & 2(q_1q_3-q_4q_2) \\ 2(q_1q_2-q_4q_3) & 1-2q_1^2-2q_3^2 & 2(q_2q_3+q_4q_1) \\ 2(q_1q_3+q_4q_2) & 2(q_2q_3-q_4q_1) & 1-2q_1^2-2q_2^2 \end{bmatrix}. \tag{11}$$

Treating the linear spring and damper in parallel, the resultant tensile force magnitude developed by the i^{th} sub-tether is:

$$F_{\mathrm{i}} = \begin{cases} k(\|\mathbf{L}_{\mathrm{i}}\| - L_0) + c[\mathbf{v}_{\mathrm{j}} - (\mathbf{v}_{\mathrm{t}} \\ \qquad +\mathbf{A}(\mathbf{q})^{\mathrm{T}}\boldsymbol{\omega}^{\times}\mathbf{r}_{\mathrm{i}})]\dfrac{\mathbf{L}_{\mathrm{i}}}{\|\mathbf{L}_{\mathrm{i}}\|}, & \text{for } \|\mathbf{L}_{\mathrm{i}}\| - L_0 > 0 \\ 0, & \text{otherwise} \end{cases} \tag{12}$$

where $\mathbf{v}_{\mathrm{j}}$, $\mathbf{v}_{\mathrm{t}}$ are velocity components of the junction and target in the inertially fixed reference frame, respectively. The tether material is assumed to have a linear spring constant, represented by k, and a damping coefficient represented by c. The resulting inertial net force on the target debris due to the sub-tethers is then given by

$$\mathbf{F} = \sum_{1}^{n} F_{\mathrm{i}}\frac{\mathbf{L}_{\mathrm{i}}}{\|\mathbf{L}_{\mathrm{i}}\|} \tag{13}$$

in the general case for n sub-tethers. This paper considers the four sub-tether configuration, where $n = 4$.

The torque imparted on the target is then

$$\mathbf{T} = \mathbf{A}(\mathbf{q})\sum_{1}^{n} F_{\mathrm{i}}\frac{\mathbf{r}_{\mathrm{i}}{}^{\times}\mathbf{L}_{\mathrm{i}}}{\|\mathbf{L}_{\mathrm{i}}\|} \tag{14}$$

which is defined in $\mathcal{F}_{\mathrm{B}}$. To solve the dynamics of the system, Eq. 14 and Eq. 13 are used with the governing equations of motion, Eqs. (5) to (8), for the appropriate bodies.

4. NUMERICAL SIMULATIONS

To determine the feasibility of the proposed novel tethered configuration to control the attitude of an uncooperative and spinning debris, numerical simulations were performed.

Assuming a short time-scale, the gravitational field effects will cause negligible relative motion between the two spacecraft and is therefore ignored. The tether is modeled as a massless single link (i.e., no torsion or bending effects). The tethers are assumed to be perfectly attached to the debris at its extremities as shown in Fig. 1.

The tether material chosen to model is Technora for its low density, high strength, and resistance to UV and atomic oxygen degradation[1], making it a suitable material for a TSS. Technora has a Young's Modulus of 70 GPa. The spring constant of a tether is given by:

$$k = \frac{EA}{L} \tag{15}$$

where E is the Young's Modulus, A is the cross sectional area, and L is the tether length. For a 20 meter tether with a diameter of 10 mm, the spring constant is, this yields:

$$k \approx 275 \, \frac{\mathrm{kN}}{\mathrm{m}}.$$

Four cases are investigated. Case 1 simulates capturing a nominally spinning debris, where the chaser is passive after capture. Case 2 shows the resulting motion when the chaser captures a tumbling debris and remains stationary after capture, i.e., simulating the capture of a small debris. Case 3 simulates the effects of capturing a debris and commanding the chaser to thrust away from the debris, effectively maintaining tension and towing the debris. Case 4 simulates a passive technique for controlling the attitude of the debris. That is, to rotate the TSS about its barycenter as a means of generating tether tension.

The simulations are performed using an Adams integration scheme over 100 seconds, using a 0.1 second output time step. In each case, the target has initial angular rates of:

$$\boldsymbol{\omega} = \begin{bmatrix} 0.5 \\ 0.5 \\ 0.5 \end{bmatrix} \frac{\mathrm{rad}}{\mathrm{s}}.$$

Output graphs show the resulting angular rates of the target vs time, in order to determine whether the target's initial angular rates are being damped out. Another important result is the separation distance between the chaser and the target as a function of time. The relative position plots have a shaded region denoted "collision zone" (for relative positions less than 15 m), which within there is a high risk of collision and mission failure.

4.1. Case 1 - Passive Chaser

A debris is captured at $t = 0$ when it is initially tumbling. Table 1 contains the initial conditions and TSS properties of the simulation. The bodies are initially positioned such that all the tethers are in tension. The chaser performs no action after the target is captured. This provides a sense of the natural tendencies of the system.

The resulting target attitude motion, as described by the angular rates, is shown in Fig. 3. Initially, the sub-tethers reduce the angular rates of the target. However, in doing so, a portion of the target's angular momentum is converted into linear momentum. This causes the debris and chaser to drift toward each other. As the translational motion begins, all tethers become slack (i.e., no forces are imparted on the target and angular and linear momentum are conserved). Eventually, the debris and chaser collide with each other, as illustrated by the shaded collision zone in Fig. 4. This shows that depending on the initial conditions, inaction after capture may lead to a mission failure. Therefore, other alternatives must be analyzed.

[1]Technora material properties obtained from `http://www.teijin.com/products/advanced_fibers/aramid/contents/aramid/technora/eng/technora_top_e.html`

Table 1. Initial conditions and TSS parameters for Case 1 simulation.

Parameter	Value
I_{xx} [kg m^2]	2500
I_{yy} [kg m^2]	2500
I_{zz} [kg m^2]	5000
m_{t} [kg]	2500
m_{j} [kg]	1
m_{c} [kg]	3000
$\mathbf{r_t}(1)$ [m]	$[0, 0, 0]^T$
$\mathbf{r}_{\mathrm{j}}(1)$ [m]	$[0, 0, 21.9]^T$
$\mathbf{r_c}(1)$ [m]	$[0, 0, 41.9]^T$
$\mathbf{v_t}(1)$ $[\frac{\mathrm{m}}{\mathrm{s}}]$	$[0, 0, 0]^T$
$\mathbf{v_j}(1)$ $[\frac{\mathrm{m}}{\mathrm{s}}]$	$[0, 0, 0]^T$
$\mathbf{v_c}(1)$ $[\frac{\mathrm{m}}{\mathrm{s}}]$	$[0, 0, 0]^T$
L_{main} [m]	20
L_{sub} [m]	20
k $[\frac{\mathrm{kN}}{\mathrm{m}}]$	275
c $[\frac{\mathrm{Ns}}{\mathrm{m}}]$	10
F [N]	0
Debris Size [m]	[10,10,5]

4.2. Case 2 - Stationary Chaser

A debris is captured at $t = 0$ when it is initially. Table 2 contains the initial conditions and TSS properties of the simulation. Here, the chaser mass is large such that it effectively remains stationary after the target is captured. This could be for the case where $m_{\mathrm{c}} \gg m_{\mathrm{t}}$, or where an active control system is implemented on the chaser such that it remains stationary.

This simulation has very similar results to that of Case 1. That is, the angular momentum of the target is rapidly converted into linear momentum in the direction of the chaser. The tethers become slack and a collision occurs. The collision occurs slower than in Case 1 because the chaser is stationary. Case 1 and Case 2 show that chaser action may be necessary to avoid collision.

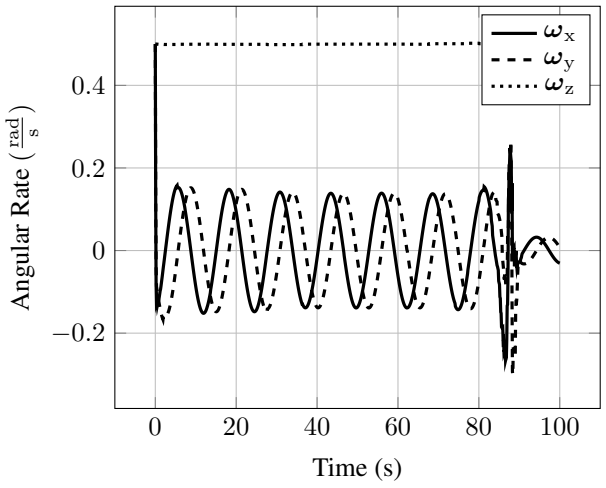

Figure 3. Target angular rates as a function of time, when initially tumbling and chaser is inactive after capture.

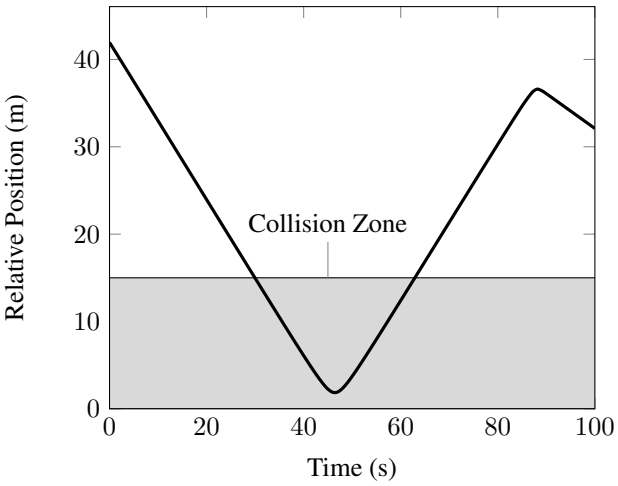

Figure 4. Relative position of chaser from target, when initially tumbling and chaser is inactive after capture.

4.3. Case 3 - Constant Thrust

This case involves the thrust capabilities of the chaser, such that it is continuously thrusting away from the target. Initial conditions and TSS parameters are shown in Table 3, and are chosen such that all tethers are initially in tension.

Fig. 7 shows that in the presence of a thrust force on the chaser, the angular rates of the target can be controlled. Note the angular rates in the x and y axes approach zero, although they do not reach zero. Due to the nature of this sub-tether configuration, there is a non-zero angular separation between when one sub-tether becomes tight and when an opposite sub-tether becomes tight. Therefore, small scale oscillations will be present in the long term.

Discontinuities are present in Fig. 7 every few seconds which correspond to the tethers becoming tight. Notice how the discontinuities coincide with local maximums of Fig. 8, which illustrates the relative position of the two spacecraft as a function of time. The z axis (also the axis of the main tether) rate has a short transient but settles back to its initial value. This indicates that the debris cannot be controlled along the main tether axis. Therefore, if a net is thrown over the debris as a means of attaching the tethers to the debris, this result has implications on the direction that the net should be launched from. That is, the net should be thrown such that the main tether axis coincides with the target axis of least angular momentum. In the desire to maximize the dissipation of angular momentum from a spinning debris, this is a key consideration.

Table 2. Initial conditions and TSS parameters for Case 2 simulation.

Parameter	Value
I_{xx} [kg m^2]	2500
I_{yy} [kg m^2]	2500
I_{zz} [kg m^2]	5000
m_{t} [kg]	2500
m_{j} [kg]	1
m_{c} [kg]	large
$\mathbf{r_t}(1)$ [m]	$[0,0,0]^T$
$\mathbf{r_j}(1)$ [m]	$[0,0,21.9]^T$
$\mathbf{r_c}(1)$ [m]	$[0,0,41.9]^T$
$\mathbf{v_t}(1)$ [$\frac{\mathrm{m}}{\mathrm{s}}$]	$[0,0,0]^T$
$\mathbf{v_j}(1)$ [$\frac{\mathrm{m}}{\mathrm{s}}$]	$[0,0,0]^T$
$\mathbf{v_c}(1)$ [$\frac{\mathrm{m}}{\mathrm{s}}$]	$[0,0,0]^T$
L_{main} [m]	20
L_{sub} [m]	20
k [$\frac{\mathrm{kN}}{\mathrm{m}}$]	275
c [$\frac{\mathrm{Ns}}{\mathrm{m}}$]	10
F [N]	0
Debris Size [m]	[10,10,5]

Safe separation distances are maintained throughout the stabilizing process, as shown in Fig. 8. There are small oscillations in relative position, which are expected due to the energy storage capabilities of the tethers. However, due to the damping properties of the tethers, these oscillations decay over time such that the steady-state separation distance is extended from its initial value by

$$s_{ss} = \frac{F}{k}$$

where s_{ss} is the steady-state stretch in the tethers, k is the spring constant of the tethers, and F is the thrust magnitude applied by the chaser.

This case is the first in this paper to demonstrate the feasibility of the modified TSS as a means for dissipating the angular momentum of the debris after capture.

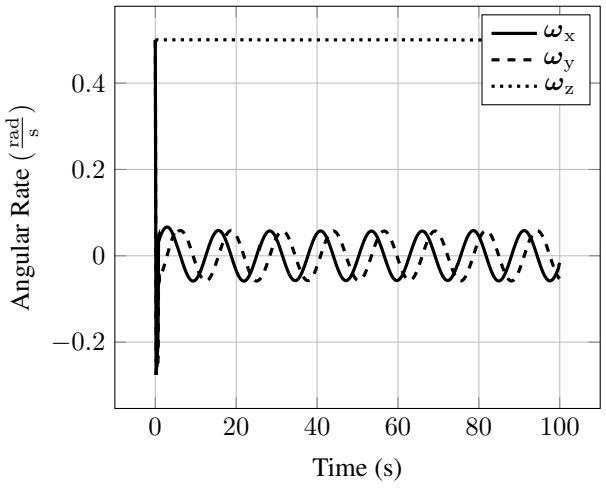

Figure 5. Target angular rates as a function of time, when initially tumbling and chaser is stationary after capture.

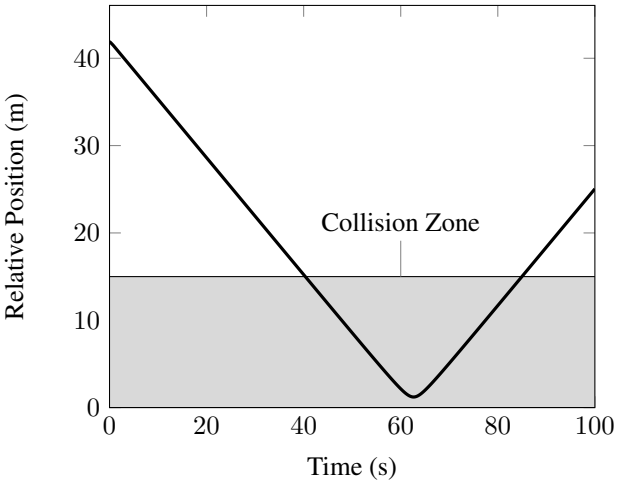

Figure 6. Relative position of chaser from target, when initially tumbling and chaser is stationary after capture.

4.4. Case 4 - Barycenter Rotation

Another mode for preventing collision, and maintaining tension in the tethers sufficient for controlling the attitude of the debris, is to rotate the chaser and the debris around each other (i.e., rotating the TSS about its barycenter). Initial velocities are imparted to each body, as listed along with the TSS properties in Table 4.

This case demonstrates another stable mode of motion after capture. That is, a controlled rotation rate along two axes (rather than attempting to bring them to zero). This yields predictable and passive target attitude motion, once the chaser and target have begun rotating. The peaks of the oscillations on the ω_x and ω_y axes have steady-state magnitudes

$$B_{ss} = \frac{2\pi}{T}$$

where B_{ss} is the magnitude of the steady state body oscillations of the target and T is the rotational period of the TSS about its barycenter. The steady state frequency for the ω_x and ω_y oscillations is

$$f_{ss} = \frac{\omega_z}{2\pi}$$

as confirmed by Fig. 9.

A significant advantage of this control technique is that it does not require any thrust other than that to initiate the spin. This may reduce the complexity of the angular momentum dissipation process.

Table 3. Initial conditions and TSS parameters for Case 3 simulation.

Parameter	Value
I_{xx} [kg m^2]	2500
I_{yy} [kg m^2]	2500
I_{zz} [kg m^2]	5000
m_t [kg]	2500
m_j [kg]	1
m_c [kg]	3000
$\mathbf{r_t}(1)$ [m]	$[0,0,0]^T$
$\mathbf{r_j}(1)$ [m]	$[0,0,21.9]^T$
$\mathbf{r_c}(1)$ [m]	$[0,0,41.9]^T$
$\mathbf{v_t}(1)$ [$\frac{m}{s}$]	$[0,0,0]^T$
$\mathbf{v_j}(1)$ [$\frac{m}{s}$]	$[0,0,0]^T$
$\mathbf{v_c}(1)$ [$\frac{m}{s}$]	$[0,0,0]^T$
L_{main} [m]	20
L_{sub} [m]	20
k [$\frac{kN}{m}$]	275
c [$\frac{Ns}{m}$]	1000
F [N]	$[0,0,150]^T$
Debris Size [m]	[10,10,5]

5. DISCUSSION

Case 1 and Case 2 show that if the chaser does not react after capturing the debris, the passive satellite attitude is not controlled and a collision between the target and the chaser may occur. Therefore, two cases are investigated to avoid collision and stabilize the passive and tumbling satellite. Case 3 proposes to use the chaser's thrusters continually to avoid collision. The use of thrusters successfully demonstrates the feasibility of this configuration of the TSS to safely control a passive satellite. The resulting angular rates along the two transverse axes approach zero due to the damping nature of the tether material. However, the angular rates along the tether axis are not controlled by the TSS. Case 4 is also a proposed passive solution to the control of the passive satellite after capture. It consists of the chaser and target to have

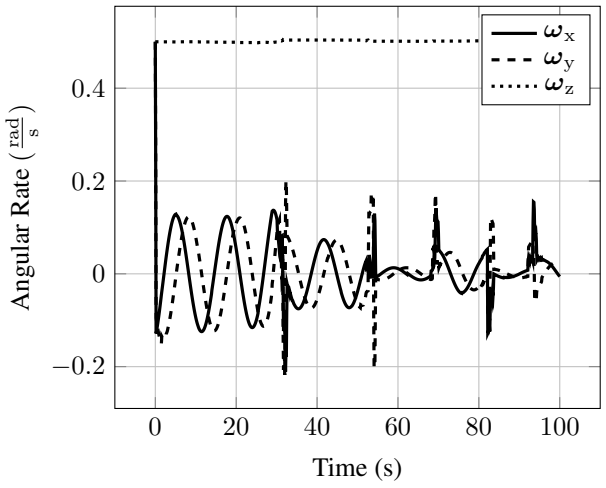

Figure 7. Target angular rates as a function of time, when target is initially tumbling and chaser thrusts away from the target.

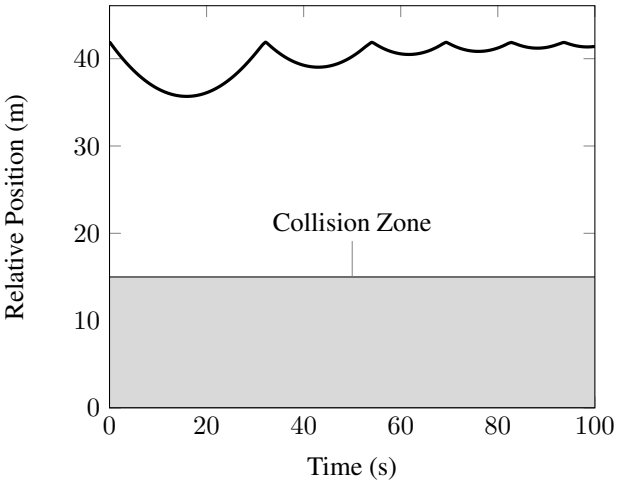

Figure 8. Relative position of chaser from target, when target is initially tumbling and chaser is thrusting away from target.

linear velocity in opposite directions such that the TSS rotate around its barycenter. The centrifugal force maintains tension in the tethers, which avoids collision and stabilizes the target as shown in Fig. 9 and 10.

6. CONCLUSION

A novel Tethered Satellite System (TSS) where the main tether attached to the chaser branches into four sub-tethers that are attached to a tumbling passive satellite was proposed and analyzed. A Newtonian dynamics formulation was performed to investigate various modes of attitude control of the passive satellite through the use of visco-elastic sub-tethers and thrusters on the chaser. Four simulations were performed, each initially with the tethers tight and the target tumbling. It was found that initial angular motion of the target about all three axes, without any thrust use on the chaser, leads to a collision. To avoid a collision, two options were investigated. First, using the thrusters on the chaser, directed away from the target, can be used to prevent collision and also dissipate most of the angular momentum of the target. Another control mode is to spin the TSS around its barycenter such that the centripetal force generated by the tether regulates the target attitude and collision is prevented.

Table 4. Initial conditions and TSS parameters for Case 4 simulation.

Parameter	Value
I_{xx} [kg m^2]	2500
I_{yy} [kg m^2]	2500
I_{zz} [kg m^2]	5000
m_t [kg]	2500
m_j [kg]	1
m_c [kg]	3000
$\mathbf{r_t}(1)$ [m]	$[0,0,0]^T$
$\mathbf{r_j}(1)$ [m]	$[0,0,21.9]^T$
$\mathbf{r_c}(1)$ [m]	$[0,0,41.9]^T$
$\mathbf{v_t}(1)$ [$\frac{m}{s}$]	$[0,3,0]^T$
$\mathbf{v_j}(1)$ [$\frac{m}{s}$]	$[0,0,0]^T$
$\mathbf{v_c}(1)$ [$\frac{m}{s}$]	$[0,-3,0]^T$
L_{main} [m]	20
L_{sub} [m]	20
k [$\frac{kN}{m}$]	27.5
c [$\frac{Ns}{m}$]	1000
F [N]	0
Debris Size [m]	[10,10,5]

An important result from the two successful methods for controlling the target is the angular momentum along the main tether axis (i.e., the axis facing the chaser) cannot be controlled. This is due to the lack of a moment arm about this axis. If a mission were being designed to capture a tumbling debris, this result indicates that the debris should be approached along its axis of least angular momentum.

Future work will focus on the development of an adaptive control system for implementation on the chaser spacecraft. To validate the dynamics and control system performance, three degree-of-freedom experiments using free-floating air-bearing spacecraft platforms maneuvering on a large granite surface at the Spacecraft Robotics and Control Laboratory at Carleton University will be performed.

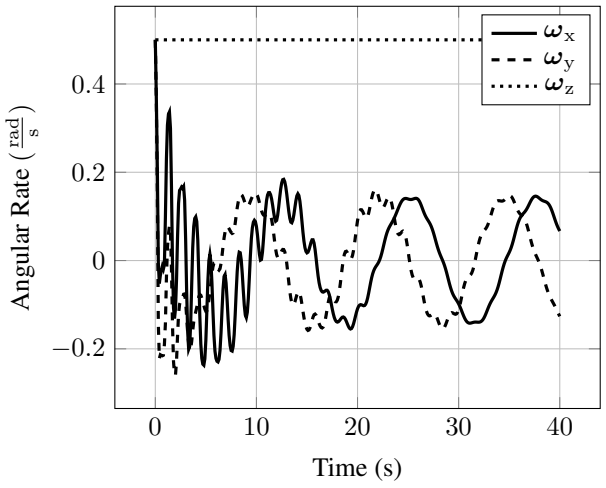

Figure 9. Target angular rates as a function of time, when target is initially tumbling and the TSS is rotating.

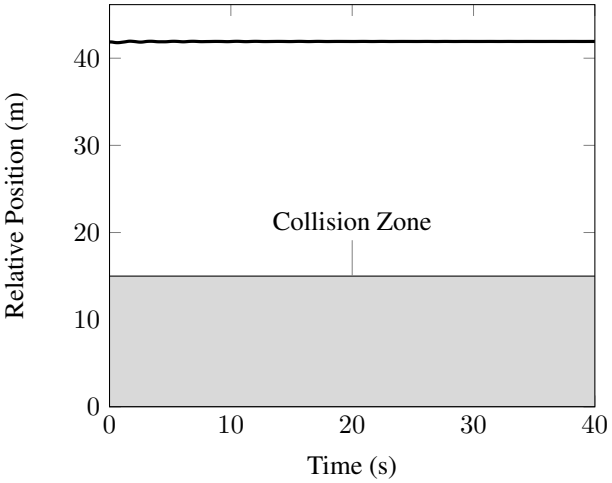

Figure 10. Relative position of chaser from target, when target is initially tumbling and both bodies are spinning around each other.

ACKNOWLEDGMENTS

The author would like to thank Bruce Burlton for his guidance and motivation on this research.

REFERENCES

[1] Jasper, L. E. Z., Seubert, C.R., Schaub, H., Valery, T., and Yutkin, E., "Tethered Tug for Large Low Earth Orbit Debris Removal," *AAS/AIAA Astrodynamics Specialists Conference*, AAS/AIAA, Charleston, SC, Feb. 2012, AAS 12-252.

[2] Kaplan, M.H., Boone, B., Brown, R., Criss, T.B., and Tunstel, E.W., "Engineering Issues for All Major Modes of In Situ Space Debris Capture," *AIAA Space 2010 Conference & Exposition*, AIAA, Anaheim, CA, Sept. 2010, AIAA 2010-8863.

[3] Alpatov, A. P., Beletsky, V. V., Dranovskii, V. I., Khoroshilov, V. S., Pirozhenko, A. V., Troger, H., Zakrzhevskii, A. E., *Dynamics of Tethered Space Systems*, Taylor & Francis, Boca Raton, FL, 2010

[4] Aslanov, V. S. and Yudintsev, V. V., "Dynamics of large debris connected to space tug by a tether," *Journal of Guidance, Control and Dynamics*, Vol. 36, No. 6, 2013, pp. 1654-1660.

[5] Aslanov, V. S., Yudintsev, V. V., "Dynamics, Analytical Solutions and Choice of Parameters for Towed Space Debris with Flexible Appendages," *Advances in Space Research 55*, 2015, pp. 660-667.

[6] Aslanov, V. S., Yudintsev, V. V., "Behavior of Tethered Debris With Flexible Appendages," *Acta Astronautica*, Vol. 104, No. 1, 2014, pp. 91-98.

[7] Aslanov, V. S., Yudintsev, V. V., "Dynamics of large space debris removal using tethered space tug," *Acta Astronautica*, Vol. 91, 2013, pp. 149-156.

[8] Aslanov, V. S., and Ledkov, A. S. "Dynamics of towed large space debris taking into account atmospheric disturbance," *Acta Mechanica*, Vol. 225, No. 9, 2014, pp. 2685-2697.

[9] Hughes, P., *Spacecraft Attitude Dynamics*. Dover Publications, Mineola, NY, 2004, pp. 17-18, 58-59.